Spring 2018

Transmission line inspection using suspended robot: Cost effective analysis and operational routing identification

Balaji Rathinam Nagarajan

TRANSMISSION LINE INSPECTION USING SUSPENDED ROBOT: COST EFFECTIVE ANALYSIS AND OPERATIONAL ROUTING IDENTIFICATION

by

BALAJI RATHINAM NAGARAJAN

A THESIS

Presented to the Faculty of the Graduate School of the

MISSOURI UNIVERSITY OF SCIENCE AND TECHNOLOGY

In Partial Fulfillment of the Requirements for the Degree

MASTER OF SCIENCE IN ENGINEERING MANAGEMENT

2018

Approved by

Dr. Zeyi Sun, Advisor

Dr. Ruwen Qin

Dr. Abhijit Gosavi

ABSTRACT

High voltage transmission lines form a crucial part of the energy infrastructure of a country. Effective maintenance is required to maintain its reliability and reduce the probability of the occurrence of the outage. Conventionally, the routine inspection of the transmission line was conducted by linemen with the assistance of hot stick and helicopter, which is considered dangerous, time-consuming, and expensive.

In this thesis, we focus on the initial study of seeking the state of the art robotics technology to by largely replace human beings in transmission line inspection. The existing robotics technologies that are interested by utility companies, as well as the background information of transmission system, are first briefly reviewed. The motivation and objective of the thesis are given. Then, a cost model for using a suspended robot in transmission line inspection following a heuristic routing strategy that guides the motion of the ground support team is introduced. Numerical case study considering various terrain characteristics is implemented to demonstrate the cost related performance of the inspection task using the suspended robot. After that, a revised A-Star routing algorithm is derived to identify the travel path of the ground team to reduce the travel time and distance to further improve the cost-effectiveness of using the suspended robot in transmission line inspection. A true segment of transmission line in Missouri (MO) is used in case study to illustrate the effectiveness of the derived routing algorithm. Finally, the conclusion of the thesis is drawn, and the future work is discussed.

ACKNOWLEDGEMENTS

I am very grateful to my advisor, Dr. Zeyi Sun, for his continuous support and belief in me. His advice has led me to the right way.

I would like to extend my appreciation to the committee members, Dr. Ruwen Qin and Dr. Abhijit Gosavi for their valuable feedback about this thesis.

I am thankful to Ameren for funding this research and providing various other important data related to this study.

Finally, I would like to thank my parents and well-wishers. Without their support, I wouldn’t be able to reach this far.

TABLE OF CONTENTS

LIST OF ILLUSTRATIONS

LIST OF TABLES

1. INTRODUCTION

High voltage transmission lines connecting the power plants and sub-stations located near the load (How electricity is delivered to consumers, n.d.) form a vital part of delivering power from the source to the customer. It is one of the key factors in determining the reliability of the power infrastructure in a country. Various components are involved in the transmission system. They need to be well maintained according to given safety and reliability standards under a harsh environmental condition. The potential damages and degradations caused by poor weather and long-term use could lead to the incomplete functioning of the components (Overhead Distribution Manual, n.d.), which could result in power loss and poor service to the customers.

1.1. TRANSMISSION LINE COMPONENTS

The most important components that form the part of the transmission and distribution network are conductors, insulator, spacer, damper, and splice. Conductors are the bare wire on the line that are made of aluminum (either plain or reinforced with steel, or composite materials) as shown in Figure 1.1 (a) (Dave, n.d.; Trash, 2003). Insulators as shown in Figure 1.1 (b) are the devices made of porcelain, glasses, or polymers. They are used to contain, support, or separate electrical conductors on high voltage electricity supply networks (Molburg, Kavicky & Picel, 2008). As more than one conductors are involved in a network, components of the spacer as shown in Figure 1.1 (c) is employed to prevent the lines from touching one another due to wind or any other external vibrations (Edkins, 2008). Dumbbell-shaped devices as shown in Figure 1.1 (d) are also installed throughout the lines to suppress the wind induced vibrations and prevent the abrasions on support structures (Vibration Damper for Transmission Lines, n.d.). The transmission line is a series of conductors held together by splice that is an electric connector as shown in Figure 1.1 (e). It is soldered such that the power conducted from the source cable to the next cable is transferred at an acceptable conductivity and pull-put resistance performance level (Overhead Line Splices Automatic Copper, n.d.). The steel structures or pylons holding the components are protected against lightning by a ground wire fixed at top of each structure (The parts of a power line, n.d.).

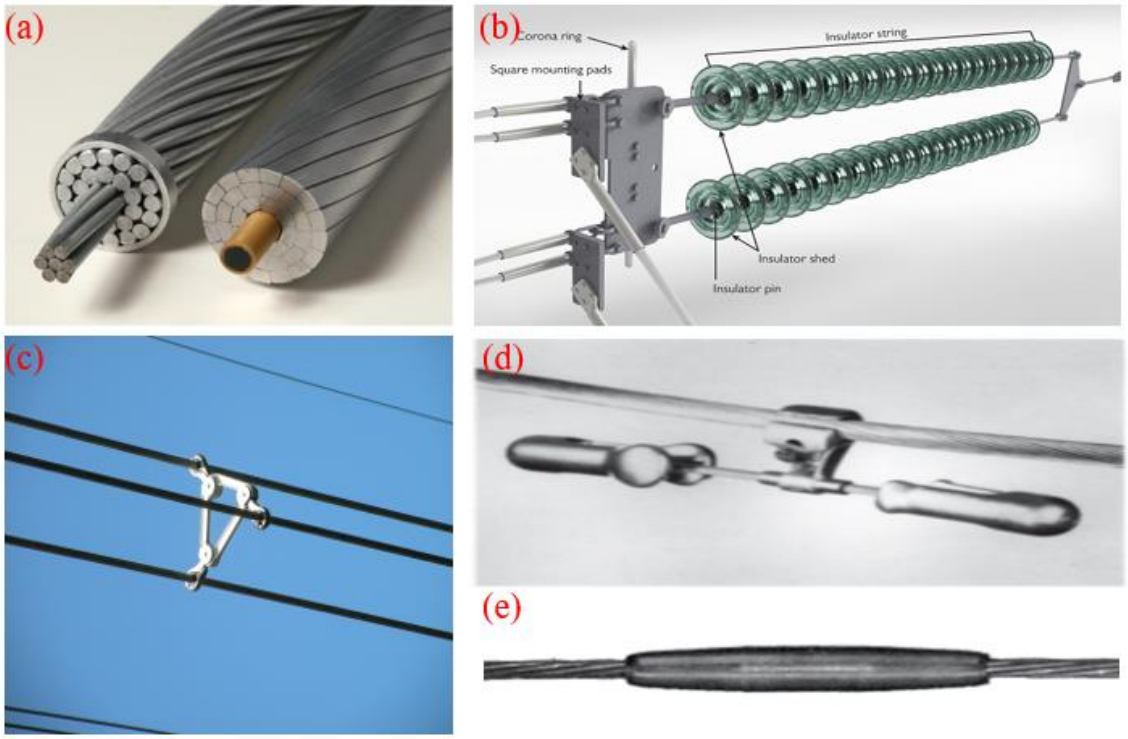

Figure 1.1. Major Transmission Line Components. (a) Conductor (b) Insulator (c) Spacer (d) Damper (e) Splice

Since most of the transmission lines are made of aluminum and steel, possible degradations as shown in Figure 1.2 due to the harsh environment and poor weather must be timely detected for having a prominent level of reliability (Liu, Cruzat & Kopsidas, 2017). In addition, the vegetation encroaching near the transmission line also needs to be monitored and chopped down if necessary (DOE, 2015). Conventional ways for the inspection of the transmission lines highly involve human interference with the use of the hot sticks on the line (Rego, Santos, & Conceicao, 2014). The inspection operation is a complicated task involving expensive processes, primarily related to the use of helicopters or any special vehicles, complex sensors, and other detection systems (Beltran et al., 2006). Meanwhile, the safety of the working personnel involved in the on-field operations must be ensured. As the requirements of reliabilities increase, limitations of employing linemen,

such as strong safety concern, energy supply interruption, weather constraint, low inspection speed, and others have been gradually recognized (Roncolatto et al., 2010).

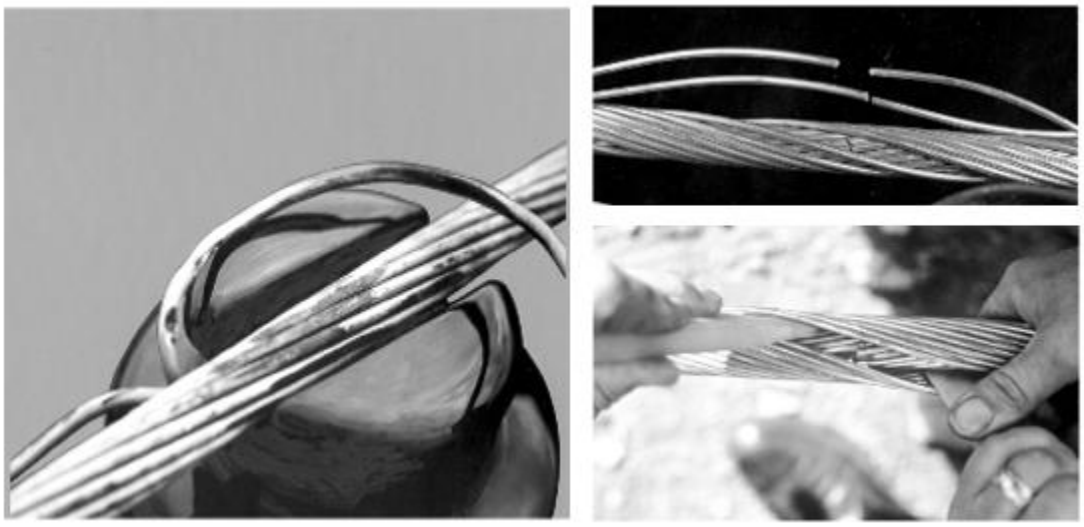

Figure 1.2. Damages to the Transmission Line due to Abrasions, Fatigue, and Weathering

1.2. ROBOTIC TECHNOLOGY FOR INSPECTION

After the fast development of the technologies in sophisticated appliances and teleoperated devices, robotics has been considered a promising alternative to replace the linemen when implementing transmission line inspection to a certain extent. The potentials of this technology were realized initially during the 1990s (Boyer, 1996; Faucher et al., 1996). Many of the live-line tasks such as infrared and visual inspection, evaluating the condition of conductor erosion and compression splices, and replacement of insulator components and overhead ground wire have been carried out with the help of robots. The robotics technologies currently developed and used in the power sector can be divided into three groups: Land based, aerial based, and suspended based robots (Elizondo, Gentile, Candia & Bell, 2010).

The land based robots usually involve trucks or cranes combined with hydraulic functionality to do the heavy lifting and/or structural supporting job. The insulated boom trucks, for example, will allow linemen to access a considerable number of line components from a fixed position (Elizondo, Gentile, Candia & Bell, 2010).

The aerial based robot is also referred to as unmanned aerial vehicles (UAVs) used for inspecting the health conditions of conductors and other components (Elizondo, Gentile, Candia & Bell, 2010). It is controlled by radio with geographical position system to ease the inspection process for improving the reliability of the transmission lines.

The suspended from line based robots (Montambault & Pouliot, 2003) are designed to travel on the transmission line. They are equipped with sensors and cameras to execute inspection and minor repair autonomously on the line by acting as eyes and hands of the linemen from a distance. The minor repairs such as fixing broken conductor strand or tightening the bolt of a spacer are carried out depending on the functionality of the robot (Koike et al., 2016).

In this thesis, we focus on the use of the suspended based robot in transmission line inspection. The suspended based robot generally is a semi-autonomous tele-controlled device which can perform basic functions such as motion and data transmission according to the whim of the linemen. The visual camera is usually equipped and connected to the onboard electronics and antennas of robot so that the live video stream showing the real-time situation of the conductor wire being inspected can be transmitted to the team on the ground while the robot is motioning along the line (Pouliot, Latulippe & Montambault, 2009; Pouliot, Mussard & Montambault, 2012). The live data transmission between the robot and the ground support team is limited by a certain range. This constraint leads to the requirement of deploying the ground support team at distinct locations so that the robot could be within the required data transmission range.

Separate tools such as electric wrench arm can be attached to the robot so that multi-functional operations like installing clamps on broken strands (Song, Wang, Jiang & Ling, 2012; Pouliot & Montambault, 2009), and measuring compression splice can be performed. To make the robot more autonomous (Peungsungwal et al., 2001), Lidar sensor can be equipped (Richard, Pouliot & Montambault, 2014; Montambault, Pouliot & Lepage, 2012) to help the robot sense and overcome some of the expected obstacles such as warning

spheres (Campos et al., 2002) on the route of the inspection trip. Robot's geometry is updated and continuously improved so that better maneuverability and speed can be attained (Pouliot & Montambault, 2008).

It has been reported that the technology of the suspended robot has been actively studied in academia and industries since the last few decades (Sawada et al., 1991; Wu, Zheng, Xiao & Li, 2009). For example, robots such as "Ti" developed by the Electric Power Research Institute as shown in Figure 1.3 is in the development stage (Phillips, Engdahl, McGuire, Major & Bartlett, 2012). Continuous efforts are made to make the robot more autonomous and sophisticated by adding more sensors. Robots such as "LineScout" by Hydro-Québec (Montambault, Paouliot, Toth & Spalteholz, 2010) and "Expliner" by Hibot Corp (Debenest & Guarnieri, 2010) as illustrated in Figure 1.3, are a few of the commercially available technologies in the market. The LineScout robot has been tested on field and has shown promising results (Montambault & Pouliot, 2010; Toth, Pouliot & Montambault, 2010). National Grid, a utility company in Britain, has purchased the license for using LineScout for the transmission line inspection since 2014 (Hydro-Québec and National Grid, 2014).

Figure 1.3. Robot for Transmission Line. LineScout (left), Expliner (middle) and Ti (Right)

1.3. OBJECTIVE

Despite the availability of the technology, the use of robots is limited by utility industries in present days (Montambault, Pouliot & Lepage, 2012). One major concern

from the practitioners is the cost-effectiveness of employing such an emerging technology. Cost modeling plays a critical role in decision making for utility companies (Muratori et al., 2017) as well as other various industrial practitioners (Conradie, Dimitrov, & Oosthuizen, 2016; Jiang, Walczyk, McIntyre, & Chan, 2016).

Motivated by the status-quo, the objective of this thesis is to conduct initial studies in terms of cost-effectiveness of using the suspended robot in transmission line inspection so that the large-scale substitution of the robot for the linemen can be further accelerated. The rest of the thesis is organized as follows. In Section 2, the modeling and analysis for the cost of the inspection operation using the suspended robot is executed to evaluate the cost-effectiveness of the robotic technology in transmission line inspection following a simple heuristic routing strategy to track the robot's motion on the line and the ground team when implementing inspection tasks. After that, in Section 3, a new routing algorithm using revised A-Star algorithm for the ground team is proposed to further improve the cost-effectiveness performance by reducing the ground travel distance and inspection time. Finally, in Section 4, the conclusion is drawn, and future work is discussed.

2. COST ANALYSIS

This section was previously published as "Nagarajan, B., Qin, R., Sun, Z., & Islam, M. (2017) Cost analysis for high voltage transmission line inspection using robot, in Proceedings of the American Society for Engineering Management 2017 International Annual conference 18-21 Oct. 2017".

2.1. BACKGROUND

The cost of implementing an inspection task on a transmission line is intuitively dependent on the inspection time, travel distance, etc. Also, considering the data transmission range between the robot and the ground support team as introduced in Section 1, the ground support team with the receiver station needs to dynamically alter the locations to ensure robust data transmission between the robot and ground team. Further, although advanced mobility mechanisms have been designed and integrated into the robot to guide its motion across the possible obstacles, it cannot fully guarantee zero human interference, especially in dealing with some unexpected obstacles like broken conductor cable due to lightning. Thus, a routing algorithm is needed to guide the motion of the ground team to deploy receiver stations and handle those unexpected obstacles when human interference is required.

In this section, we first introduce a simple heuristic routing algorithm to guide the motion of the ground team so that the corresponding travel distance and travel time can be formulated. Then, the cost model is derived considering various cost items based on the introduced routing algorithm. After that, a numerical case study is conducted to implement the derived cost model. Finally, conclusions are drawn.

2.2. A SIMPLE HEURISTIC INSPECTION ROUTING ALGORITHM

The inspection team on the ground consists of three members: a driver, a data collector, and a maintenance staff. The data collector oversees the data transmission between the robot and receiving station on the ground. The maintenance staff is responsible

for setting up the robot to clear the potential obstacles. The inspection team carries one spare robot battery system so that two robot battery systems can be used alternatively without interrupting the inspection task.

We first assume the inspection team moving speed on the ground is much faster than the robot inspection speed and the travel path on the ground is same as that on the line. In addition, we also assume that minor repairs on the way of robot inspection can be completed by the robot itself, and the time required for the minor repair can be ignored.

Let *r* be the range of data transmission. When the robot is set up at the start point of the line for inspection, the inspection team will move to the location that is *r* distant from the start point so that it can cover the range of *r* for both directions as shown in Figure 2.1.

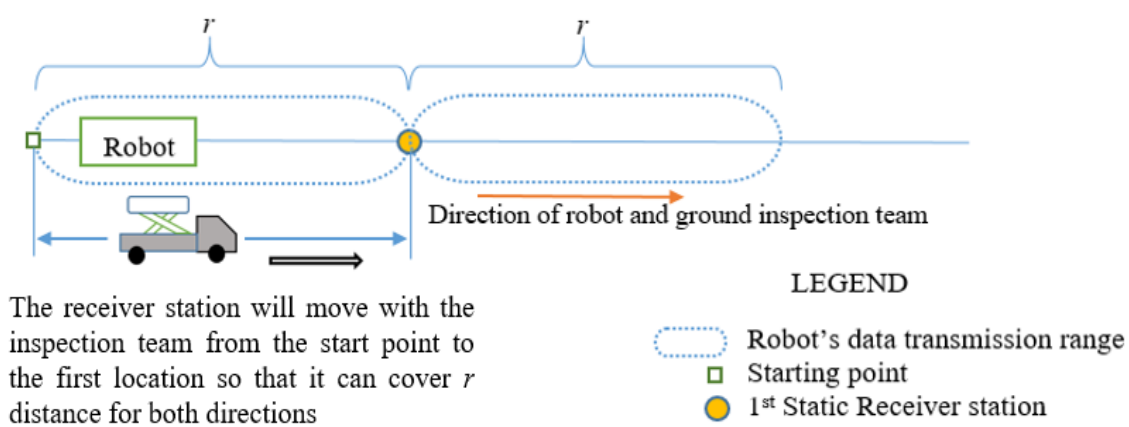

Figure 2.1. Illustration of the First Location of Receiver Station

After that, the receiving station will keep static in the place until the next moving when the robot runs out of the range of data transmission. The maintenance staff will move upon request to the obstacle places to help robot for a setup and then return to the original location during this "static" period. The inspection team will move to the next location of

receiving station with the distance of 2*r* from the current location before the robot runs out of the current range of data transmission as shown in Figure 2.2.

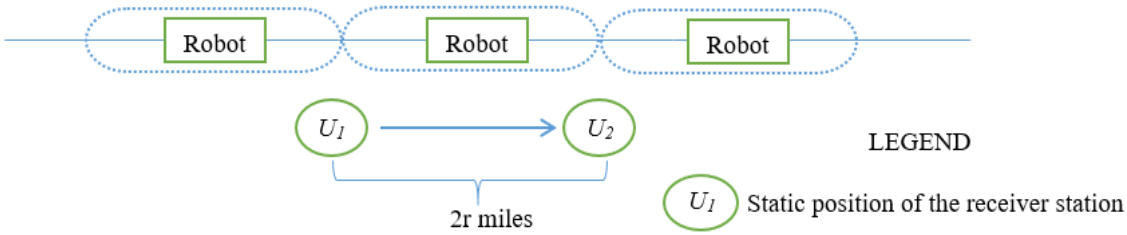

Figure 2.2. Illustration of the Motion of Receiver Station from Original Location to the Next Location

Let n_i be the number of the locations that the receiver station needs to be deployed in trip i with distance $d(i)$ according to the routing algorithm aforementioned. n_i can be calculated by

$$n_i = \lceil d(i)/2r \rceil \tag{1}$$

where $\lceil\ \rceil$ is ceiling function. Let k =0, 1, …, n_i be the index of the locations that receiver station needs to be deployed in trip i. U_k represents the kth location of receiver station. R_k is the distance between U_k and the start point. Note that U_0 is used to denote the start point of the inspection line and thus, R_0 is obviously zero. Also, let M_k be the midpoint between receiver stations U_k and U_{k+1}. Let F_k be the distance between M_k and start point. F_k can be calculated by

$$F_k = 2kr, \quad k = 0,1,2, \ ..., n_i - 1 \tag{2}$$

Similarly, M_0 is also used to denote the start point of the inspection line and thus, F_0 is zero, too.

Two exclusive scenarios regarding the distance $d(i)$ as follows need to be considered. The scenario one is the situation that the distance of the last section in the trip is larger than r but less than $2r$ as Figure 2.3 shows. Mathematically, it can be described by $\lceil d(i)/2r \rceil - d(i)/2r \le 0.5$. R_k can be calculated by

$$R_k = \begin{cases} 0, \; if \;\; k = 0 \\ r \cdot (2k-1), \; if \;\; k = 1, 2, \ldots, n_i \end{cases} \tag{3}$$

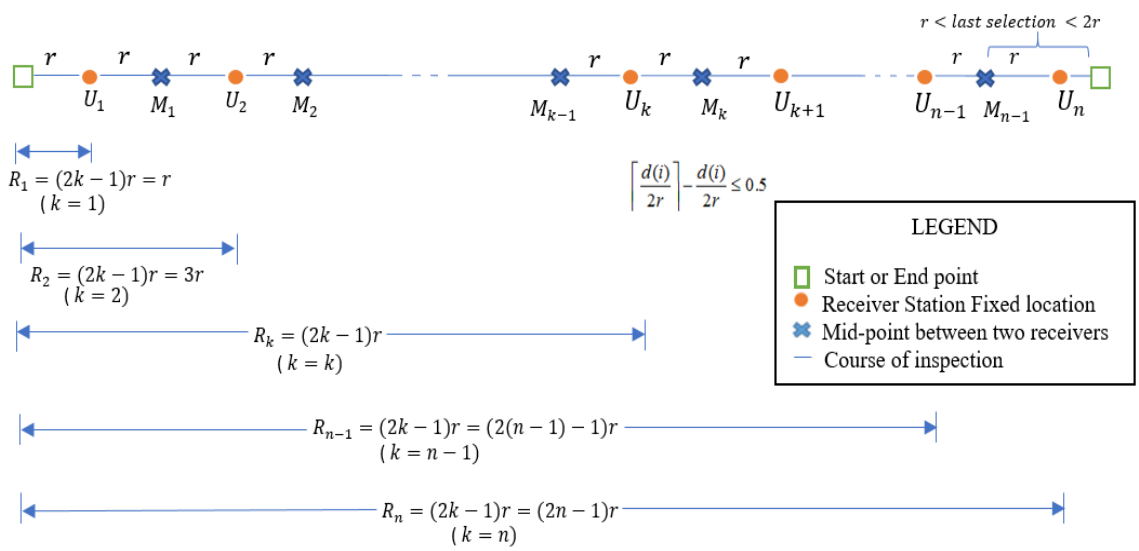

Figure 2.3. Illustration for Calculating the Distance Between Each Receiver Station Location and Start Point of the Trip in Scenario 1

Scenario 2 is the situation that the last section of the trip is less than r as shown in Figure 2.4. The figure illustrates Mathematically, it can be described by $\lceil d(i)/2r \rceil - d(i)/2r > 0.5$. R_k can be calculated by

$$R_k = \begin{cases} 0, \text{ if } k = 0 \\ r.(2k-1), \text{ if } 0 < k \le n_i - 1 \\ 2r \cdot (k-1), \text{ if } k = n_i \end{cases} \tag{4}$$

Here, in this scenario, the last station U_n is placed at r miles from U_{n-1} station unlike $2r$ miles between rest of the consecutive receiver stations.

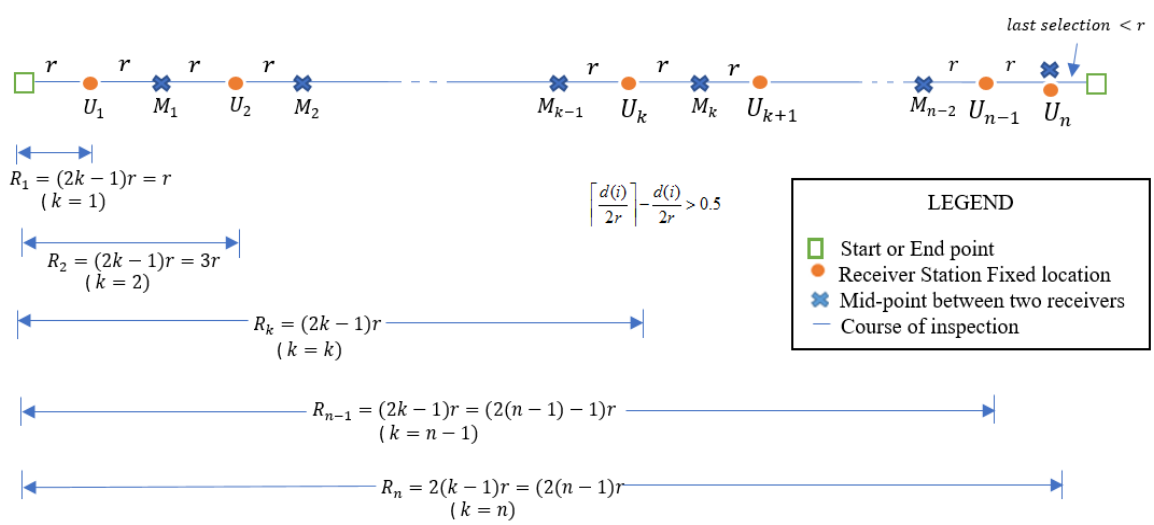

Figure 2.4. Illustration for Calculating the Distance Between Each Receiver Station Location and Start Point of the Trip in Scenario 2

The travel distance of the receiving station can be calculated as

$$R_{n_i} + (d(i) - R_{n_i}) = d(i) \tag{5}$$

where $d(i) - R_{n_i}$ is the distance between the location of receiver station and the end point of the inspection trip i. Let j=1, 2, …, $O_{d(i)}$ be the index of obstacles in $d(i)$. Let d_j be the distance between the start point and the obstacle j. The travel distance for helping robot overcome the obstacles in trip i can be formulated as

$$2 \cdot \sum_{k=0}^{n_i-1} \sum_{j \in \mathbf{J_k}} \left| R_{k+1} - d_j \right| \tag{6}$$

where $\mathbf{J_k}$ is the set of obstacle j between M_k and M_{k+1}. Thus, the total ground travel distance is

$$d(i) + 2 \cdot \sum_{k=0}^{n_i-1} \sum_{j \in \mathbf{J_k}} \left| R_{k+1} - d_j \right| \tag{7}$$

Note that we use M_{n_i} to denote the ending point of the inspection trip i.

2.3. THE COST MODEL

The total cost for inspecting a transmission line using the robot technology consists of depreciation cost considering battery depreciation, robot depreciation, data transmission system depreciation, and auxiliary equipment depreciation as well as the operation cost including team salary, ground travel, and setup as shown in Figure 2.5.

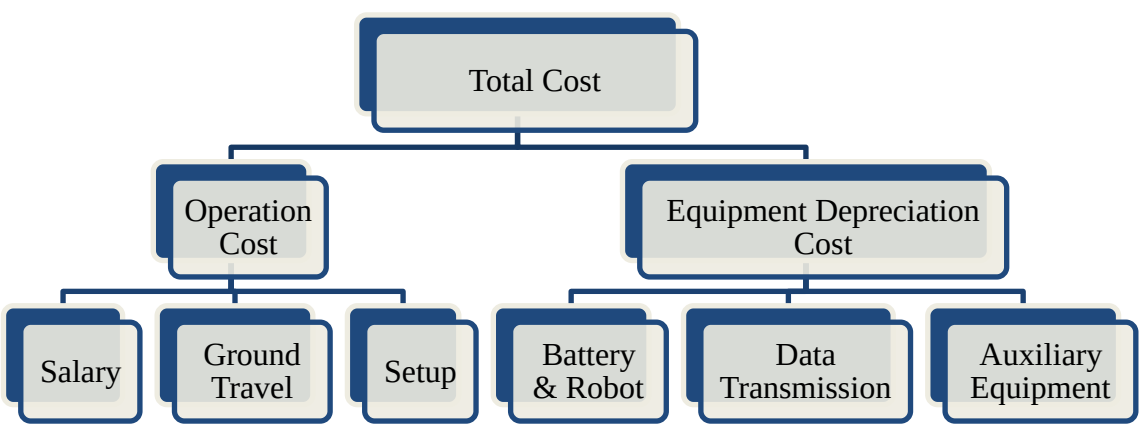

Figure 2.5. Cost Components

2.3.1. Battery Depreciation Cost (C_{bd}). There is very limited literature focusing on the battery depreciation cost for the robot used for transmission line inspection. Thus, we refer to some existing literature for the battery in electric vehicles (EV) for modeling our battery depreciation cost. The battery depreciation in EV is considered the result from the degradation of cell capacity retention with the increase of battery working cycles. It is a complex physical and chemical process influenced by many different parameters (Vetter et al., 2005). Some researchers modeled the battery degradation as a function of driving time or working cycle. It is shown that the energy capacity drop is a linear (or approximately linear) process with respect to the increase of working time (or cycle) (Ortega-Vazquez, 2013; Peterson et al., 2010). Therefore, for simplification, many studies employ such a linear degradation model to calculate the battery depreciation cost (Liu & Zhang, 2017; Zhang, Wang, & Cao, 2014; Zhang, Wang, & Wang, 2015). The ratio between the number of charging/discharging cycles (or working time) for a certain task and the expected cycles of the lifetime (or expected working time of the entire life) is used as the measure of the depreciation due to such a task. Then, the battery depreciation cost is calculated by timing this ratio with the purchase cost of the battery. In this section, we also adopt the similar method to model the battery depreciation cost considering the battery purchase cost, the expected battery lifetime (unit: number of cycles of charging/discharging), and the number of charging/discharging cycles to cover $d(i)$ inspection distance. The energy consumption of the robot for covering $d(i)$ distance can be calculated by

$$E_{d(i)} = p(i) \cdot \frac{d(i)}{v(i)} \tag{8}$$

where $p(i)$ is the average power level of the robot to keep motion on the transmission line in trip i, and $v(i)$ is average velocity of the robot when traveling through the trip i. The total energy consumption can be formulated as $\sum_i E_{d(i)}$. Since one more spare battery is carried to the inspection trip, the required number of charging for each battery can be formulated

as $\frac{1}{2}\sum_i E_{d(i)} / K$, where K is the allowed capacity of the robot battery by one charge. Thus, the battery depreciation cost can be formulated as

$$C_{bd} = 2 \cdot G_B \cdot \frac{\frac{1}{2}\sum_i E_{d(i)} / K}{L_B} = \frac{G_B \cdot \sum_i E_{d(i)}}{KL_B} \tag{9}$$

where G_B is the purchase cost for a battery system. L_B is the expected working cycle of lifetime of the battery. Note that the straight-line depreciation method with a zero salvage at the end of the service life is used here to determine the depreciation cost for batteries. This is a simple but useful method that is widely used in calculating the equipment depreciation cost (Groover, 2008; Jiang, Walczyk, McIntyre, & Chan, 2016), and thus it will also be used for calculating depreciation costs of other components in this thesis.

2.3.2. Setup Cost (C_s). Setup cost consists of the cost incurred by the initial setup to start the inspection task (C_{si}), the setup for battery replacement (C_{sc}), the setup to overcome the obstacles (C_{so}). Let $N_{d(i)}$ be the number of battery replacement to cover $d(i)$. It can be calculated as

$$N_{d(i)} = \lfloor E_{d(i)} / K \rfloor \tag{10}$$

where $\lfloor\ \rfloor$ is floor function. Let c_s be the cost per setup for battery replacement, thus C_{sc} can be formulated as follows.

$$C_{sc} = c_s \cdot \sum_i N_{d(i)} \tag{11}$$

Let $O_{d(i)}$ be the number of obstacles where the robot needs to be re-setup by human throughout the distance $d(i)$, c_s be the setup cost per required per obstacle, and C_{so} can be calculated as

$$C_{so} = c_s \cdot \sum_i O_{d(i)} \tag{12}$$

Thus, the total setup cost can be formulated as

$$C_s = C_{si} + C_{sc} + C_{so} \tag{13}$$

Note that here we actually ignored the possibility that obstacle-setup, battery replacement, and receiver station relocation can happen simultaneously. Thus, our cost model would be a progressive estimation.

2.3.3. Robot Depreciation Cost (C_{rd}). The robot depreciation cost can be calculated using the expected lifetime of the robot and the working time of robot (T) to cover the required distance of inspection. Here the time required for setup to overcome the obstacles and battery replacement is not counted. The degradation is purely from the motion time of robot in the trip.

$$T = \sum_i d(i) / v(i) \tag{14}$$

The robot depreciation cost can be formulated as

$$C_{rd} = G_R \cdot \frac{T}{L_R} \tag{15}$$

where G_R is the purchase cost of the robot; and L_R is the expected working time of the robot.

2.3.4. Salary Cost (C_{st}). The salary cost is calculated using the salary per unit time and the expected time that is required to complete the $d(i)$ distance inspection. Let s_{mt}, s_{dr}, and s_{da} be the salary rate for the maintenance, driver, and data collection staffs, respectively. Thus, the salary cost can be formulated as

$$C_{st} = (s_{mt} + s_{dr} + s_{da}) \cdot (T + T_s + T_c) \tag{16}$$

where T_s and T_c are the total setup time and final close time for the team, respectively. T_s can be calculated by

$$T_s = t_s \cdot \sum_i (N_{d(i)} + O_{d(i)}) \tag{17}$$

where t_s is the time required for each setup. We assume the setup times of battery replacement and obstacle crossing are the same.

2.3.5. Data Transmission System Depreciation Cost (C_{dd}). The depreciation of the data transmission system can be evaluated by the working time. Let the L_D be the expected working time of the data transmission system, and G_D be the purchase cost of the data transmission system. The depreciation cost can be calculated by

$$C_{dd} = G_D \cdot \frac{T + T_s}{L_D} \tag{18}$$

2.3.6. Auxiliary Equipment Depreciation Cost (C_{ae}). Auxiliary equipment may include the apparatus possessed by the receiver station and the inspection team, e.g., LCD monitor, generator, joy sticks, etc. Let e be the index for each auxiliary equipment. Let $\boldsymbol{L_e}$ be the expected working time of equipment e, and G_e be the purchase cost of the equipment e. The depreciation cost of all the related auxiliary equipment can be calculated by

$$C_{ae} = \sum_{e} G_e \cdot \frac{T + T_s}{L_e} \tag{19}$$

2.3.7. Ground Travel Cost (C_{gt}). The total ground travel cost C_{gt}, can be calculated by

$$C_{gt} = \sum_{i} c_{gt} \cdot (d(i) + 2 \cdot \sum_{k=0}^{n_i - 1} \sum_{j \in \mathbf{J_k}} \left| R_{k+1} - d_j \right|) \tag{20}$$

where c_{gt} is the ground travel cost per unit distance.

2.4. CASE STUDY

In this subsection, we build a simulation model where the proposed cost model can be implemented considering different input parameters. The variations of total cost and total time spent are examined with respect to the uncertainties of the unexpected obstacles where the human intervention is required in the inspection trip. We consider three consecutive inspection trips with different geographic characteristics. Trips 1, 2, and 3 correspond to the situations of steady incline, plain terrain, and steady decline, respectively. The distance, robot velocity, and robot power consumption for each trip are illustrated in Table 2.1.

Table 2.1. Parameters of Each Inspection Trip

i	Degree of slope	$d(i)$	$v(i)$ (mph)	$p(i)$ (Watts)
1	10-30 degree	10	1.565	325
2	0-10 degree	30	1.565	250
3	< 0 degree	6	1.565	100

It has been reported that the LineScout robot has a data transmission range of 3 miles (Pouliot, Richard, & Montambault, 2015), while Expliner has only a range of 200 meters (Debenest et al., 2008). Since the technology varies significantly depending on different robots, we assume the data transmission range in this case as 1.3 miles by taking a value around the mid between two known values from the literature. The purchase costs and expected lifetime/working times of the robot, data transmission system, battery, and auxiliary equipment are listed in Table 2.2. The auxiliary equipment we consider in this case includes industrial joysticks, sunlight readable monitor, CPU, video recorder, and generator. The corresponding detailed information of the cost and expected lifetime is provided in Table 2.3. The setup cost per obstacle, per battery replacement, battery capacity, and robot's initial setup cost are illustrated in Table 2.4. On field conditions, 85% of the battery capacity can be used for a single charging/discharging cycle and the rest 15% is reserved for contingencies. The salary rates are illustrated in Table 2.5. The close time when an inspection trip i is completed, t_c, is set to be 3 hours. The time per setup, t_s is 0.33 hours. The ground travel cost rate is assumed to be 12 per mile.

Table 2.2. Parameters for Equipment Involved in Detail

	Purchase cost ($)	Expected lifetime/working time (hours)
Robot	10000	3000
Battery	1000	1000
Data transmission system	1200	4000
Auxiliary equipment	4200	5000

Table 2.3. Parameters for Auxiliary Equipment Involved in Detail

Auxiliary equipment	Cost ($)	Expected lifetime (hours)
Industrial grade joystick	300	5000
Military grade monitor	800	5000
CPU	1500	5000
Video recorder	600	5000
Generator	1000	5000
Total	4200	5000

Table 2.4. Parameters of Battery Capacity and Setup Cost

Battery Capacity (Wh)	Initial setup cost ($)	Setup cost to clear obstacle ($)	Setup cost to replace battery ($)
1324	20	17	17

Table 2.5. Salary Rates of Working Personnel

Team member	Data collection	Driver	Maintenance
Salary rate ($/hour)	40	25	35

We consider three different scenarios regarding the frequency of obstacles in the inspection trip where human intervention is required. We assume that the number of obstacles between M_k and M_{k+1} that follows the Poisson distribution with a known mean. The parameters of each scenario are given in Table 2.6.

Table 2.6. Mean of the Number of Obstacles

Scenarios of obstacle occurrence	Mean
High frequency	0.8
Medium frequency	0.6
Low frequency	0.4

The results of the total travel distance of the ground team on the route are obtained as shown in Table 2.7. There is no overlapping of the 95% confidence intervals of distance travelled by the ground team in different scenarios. This data suggests that frequency of obstacles does have a strong impact on the distance travelled.

Table 2.7. Ground Team Travel Distance of Three Scenarios Regarding Obstacle Frequency

Scenario	Travel Distance (95% CI)			
	Trip 1	Trip 2	Trip 3	Total (mile)
High	13.58	41.98	8.85	64.42 ± 1.73
Medium	12.45	37.80	8.37	58.63 ± 1.66
Low	11.94	35.00	6.85	53.79 ± 1.33

The total time spent of each scenario is listed in Table 2.8. The absence of any overlapping strongly suggests that time spent heavily relies on the number of obstacles. Recall we assumed in our model that the motion speed of the ground team is much higher than the robot. The time required to complete the inspection trip should be mainly determined by the robot travel time. It seems to imply that a significant difference in the ground team travel distance may not necessarily lead to significant difference in total time

spent. The probable reason to explain the significant difference in Table 2.8 can be the fact that the higher the frequency of obstacles, the more the setup time will be.

Table 2.8. Time Spent for Different Obstacle Frequencies

Frequency	Time (hours)			Total (95% CI)
	trip 1	trip 2	trip 3	
High	11.05	27.46	7.79	46.31 ± 0.58
Medium	10.84	26.45	7.56	44.85 ± 0.50
Low	10.66	25.26	7.11	43.04 ± 0.38

The results of the cost of three scenarios are illustrated in Tables 2.9, 2.10, and 2.11 respectively. We can observe that there is no overlapping of the 95% confidence intervals of the total cost among any of the scenarios, which implies that the difference in total cost among three scenarios is significant. It can also be observed that salary cost seems to be the dominating cost component to the total incurred cost.

Table 2.9. Cost of High Frequency Obstacle

Cost items	Trip 1	Trip 2	Trip 3	Total (95% CI)
Battery depreciation	2.35	5.96	0.75	9.07 ± 0.24
Setup	103.3	284.63	68.16	456.10 ± 29.02
Robot depreciation	21.30	63.90	12.78	97.98 ± 0.00
Salary	1105.78	2746.20	779.72	4631.49 ± 58.05
Data transmission system depreciation	2.42	7.34	1.44	11.20 ± 0.17

Table 2.9. Cost of High Frequency Obstacle (Cont.)

Auxiliary equipment depreciation	6.76	20.54	4.03	31.34 ± 0.48
Ground travel	163.02	503.76	106.30	773.08 ± 20.77
Total Cost	1404.73	3623.35	973.18	6010.27 ± 106.41

Table 2.10. Cost of Medium Frequency Obstacle

Cost items	Trip 1	Trip 2	Trip 3	Total (95% CI)
Battery depreciation	2.20	5.37	0.68	8.25 ± 0.23
Setup	95.53	234.2	52.27	383.00 ± 25.44
Robot depreciation	21.30	63.90	12.78	97.98 ± 0.00
Salary	1084.04	2645.33	755.92	4485.30 ± 50.89
Data transmission system depreciation	2.35	7.04	1.36	10.75 ± 0.15
Auxiliary equipment depreciation	6.59	19.70	3.83	30.17 ± 0.42
Ground travel	149.47	453.70	100.49	703.66 ± 19.97
Total Cost	1358.48	3429.25	931.336	5719.06 ± 95.71

Table 2.11. Cost of Low Frequency Obstacle

Cost items	Trip 1	Trip 2	Trip 3	Total (95% CI)
Battery depreciation	2.12	4.97	0.46	7.56 ± 0.19
Setup	83.46	174.70	34.16	292.33 ± 19.10
Robot depreciation	21.30	63.89	12.78	97.98 ± 0.00
Salary	1065.91	2526.33	711.72	4303.96 ± 38.20

Table 2.11. Cost of Low Frequency Obstacle (Cont.)

Data transmission system depreciation	2.29	6.68	1.23	10.21 ± 0.11
Auxiliary equipment depreciation	6.43	18.70	3.46	28.59 ± 0.32
Ground travel	143.23	420.03	82.26	645.53 ± 16.05
Total Cost	1324.76	3215.33	846.08	5386.17 ± 72.69

2.5. CONCLUSION

In this section, we developed a cost model for the transmission line inspection using suspended robots. Different cost items, such as robot depreciation cost, staff salary cost, team ground motion cost, etc., are modeled. A simulation model is developed to model different working scenarios and estimate the variation of cost considering the random factors like the occurrence of the unexpected obstacles on the inspected lines. The section provides an initial framework for studying the cost-effectiveness of using robots for transmission line inspection for utility companies. Different depreciation cost methods can be selected by the practitioners based on their own accounting system to calculate the total cost so that it can be compared to the cost of using linemen for inspection to examine the economic feasibility.

3. A NEW ROUTING STRATEGY

3.1. BACKGROUND

The results from the Section 2 show that the salary cost of the inspection team and ground travel cost are the top two contributors to the total cost of an inspection trip using the robot. The staff salary cost was modeled as the production of salary rate and working time, while the working time to complete an inspection trip is dependent on the travel distance of the ground team that is guided by the routing algorithm. The ground travel cost highly depends on the ground travel distance that is also determined by the routing algorithm that is used to guide the travel path of the ground team.

The routing algorithm described in Section 2 represents a typical simple heuristic way adopted by the utility companies. It keeps the location of receiver station fixed until the time that the robot runs out of the range of data transmission. During such a period, the robot technician needs to commute between the receiver station and the obstacles whose sizes are beyond the clearance capability of the robot itself (i.e., the size the obstacle is too large to be crossed by the robot itself without technician's interference) to help robot clear the obstacles. This simple routing guidance strategy may lead to unnecessary travel distance and additional travel time when technician's action happens at the moment when the robot is very close to the boundary of data transmission range of the current location of receiver station. In other words, under such a situation, it could lead to a reduced travel distance and/or travel time if the receiver station could move along with the technician to the location of the obstacle and select it as the new deployment location. Also, that algorithm assumes that the travel path on the ground is exactly the projection of the transmission line overhead. This assumption may lead to a shorter travel path of the ground team when the transmission line being inspected is a straight line. However, if the transmission line consists of multiple segments not connected with the same direction, following the path of the transmission line will not necessarily lead to the shortest travel distance. In addition, not all the points on this projection can be accessed. Some of them may be in the waterbody where the receiver station cannot be deployed.

Therefore, in this section, to address such limitations of the routing algorithm aforementioned, we propose a new routing strategy using a revised A-Star algorithm that

considers the possible travel distance between the deployment locations and the obstacle locations to guide the travel of the ground support team and the relocation of the receiver station. The constraint that the travel path is the projection of the overhead transmission line is also relaxed in the revised A-Star algorithm. A numerical case study based on a true section of transmission line in Missouri is implemented to illustrate the effectiveness of the proposed algorithm. The rest of the section is organized as follows. Section 3.2 proposes the new routing strategy using revised A-Star algorithm. Section 3.3 implements the case study. The conclusion of the section is drawn in Section 3.4.

3.2. A NEW ROUTING ALGORITHM

3.2.1. Conventional A-Star Algorithm. A-Star algorithm is widely used in pathfinding among multiple nodes between starting and ending locations (Goldberg, 2007). It solves the problem by searching for the path that incurs the smallest cost among all possible ones to the goal (Boroujeni et al., 2017). The algorithm begins from a specific start node, expanding the path one step at a time until the path reaches the end node or the goal. The successive node is selected based on the estimate of the cost formulated in (21).

$$f(n) = g(n) + h(n) \tag{21}$$

where n is the index of the node on the path. $g(n)$ is the cost of the path from the start node to node n. $h(n)$ is a heuristic that estimates the cheapest cost from node n to the end node or goal. With an initial condition of the location of the first node, there can be maximally eight surrounding nodes in a two-dimension plane as shown in Figure 3.1. All the f values of these eight neighboring nodes are calculated. As per algorithm, the one with the lowest f value is chosen as the next node. Then, the surrounding nodes to this newly selected node are updated accordingly, and the corresponding g and h values are also updated. This procedure is repeated iteratively until the end node or the goal is reached on the path.

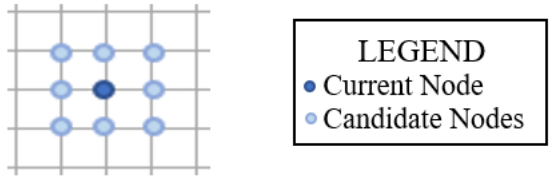

Figure 3.1. Eight Surrounding Nodes in A-Star Algorithm

3.2.2. The Revised A-Star Algorithm. With the given section of the transmission line needs to be inspected, the obstacle's locations (e.g., aerial markers with large size, structure lattice, etc.) are known to the team. The entire team with receiver station and robot starts the inspection at the start point of the transmission line. The robot is mounted on the transmission line so that it can suspend on and move forward along the inspection route. The receiver station will update its location based on the algorithm introduced as follows. Figure 3.2 shows the initial condition when the inspection starts.

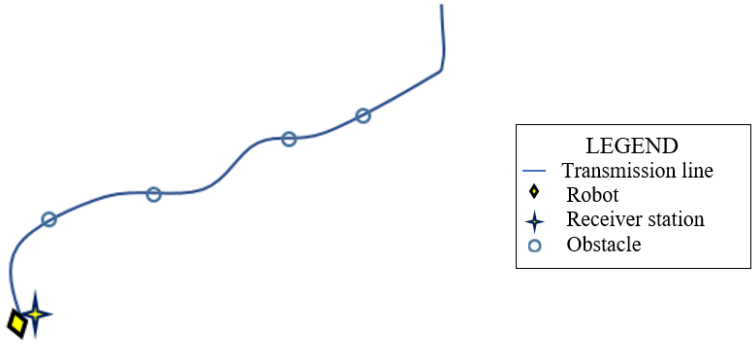

Figure 3.2. Initial Condition When Inspection Starts

Let *r* be the robot's data transmission range. With a given section of transmission line needs to be inspected, we first identify the feasible region where receiver stations can be deployed around the transmission line. The boundary of this region consists of the points whose distance to the projection of the transmission line on the ground is equal to *r*. Note that for description conciseness, we omit "projection on the ground", while only use "transmission line" to denote this projection of the transmission line on the ground in the remaining part of this section. The area that is not appropriate for deploying receiver station, e.g., the waterbody, is excluded from this feasible region. Figure 3.3 shows an example of such a feasible region.

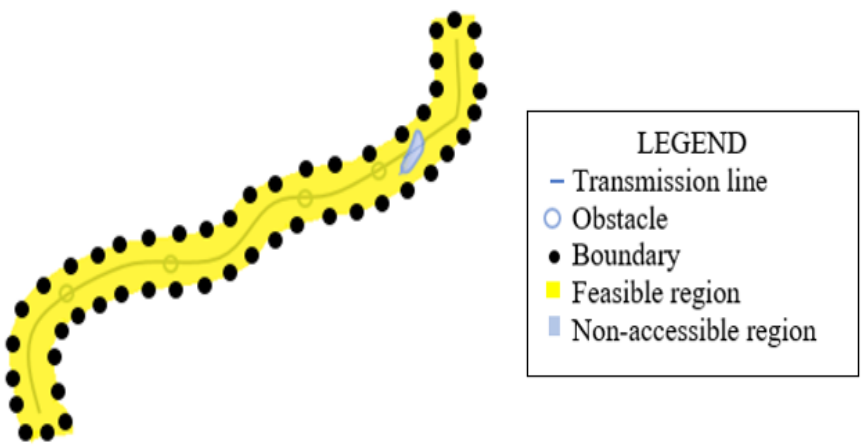

Figure 3.3. Illustration of Feasible Region

The feasible region is meshed into a set of grid nodes with a given resolution depending on the required accuracy. The receiver station will be deployed on these different nodes as well as the known obstacle points. In this section, we relax the constraint that the candidate nodes for the next deployment locations have to be confined to the eight immediately surrounding nodes as original A-Star algorithm does as shown in Figure 3.1.

Instead, a candidate area including both immediately and non-immediately surrounding nodes for the next deployment location is defined as follows.

On one hand, if the next deployment location is too close to the current one, it will lead to over-deployment. On the other hand, if the next deployment location is too far away from the current one, it will lead to the situation that a certain part of the trip of the robot may be out of the data transmittable range. Thus, the tradeoff between over-deployment and non-transmission needs to be balanced when determining such a candidate area.

To address such concerns, we first define a concentric ring area with inner and outer radiuses of l and u, respectively. For the concentric ring area, l is set as r so that the data transmission range determined by the current receiver station can be potentially maximally utilized, while u is set as $2r$ since $2r$ is the largest possible distance to which the next location that the receiver station can be deployed. It happens when the part of the transmission line is a straight line and the ground travel path is exactly the projection of the transmission line as described in Section 2 (see Figure 3.4 for illustration).

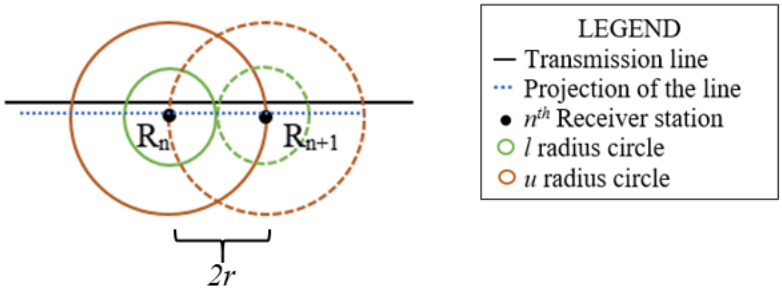

Figure 3.4. The Largest Distance Between Two Consecutive Receiver Stations

Then, we find the intersection area between this concentric ring area and the feasible region as shown in Figure 3.5. We call this intersection area as intersection area I. After that, we will find the candidate area where all the candidate nodes for the next receiver station deployment are located based on intersection area I as follows.

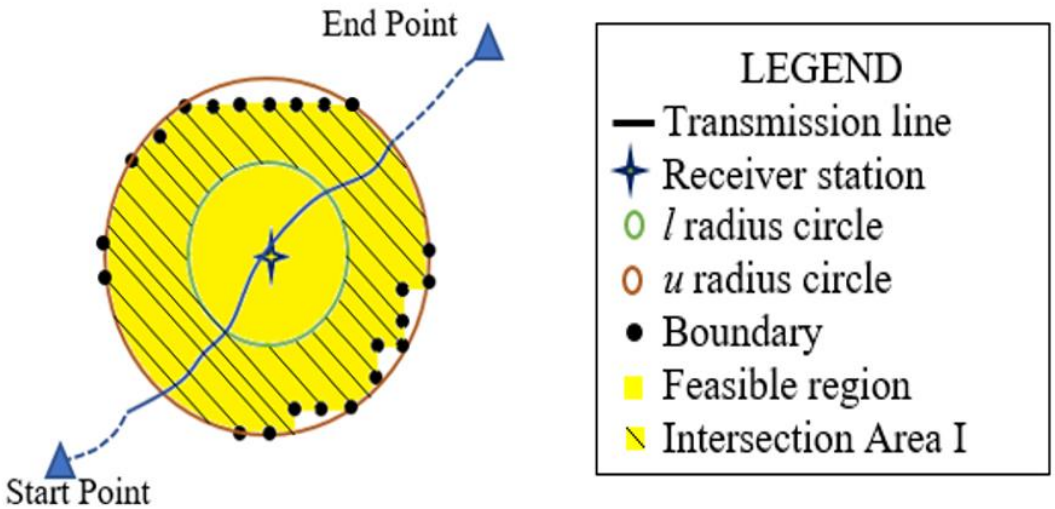

Figure 3.5. Illustration of Intersection Area I

By a given resolution, we can generate a set of points on the transmission line. The Cartesian coordinates of these points, as well as the known obstacle points, will form an $N\times2$ matrix to store the two-dimension Cartesian coordinates (x, y) of all the points. The 1st and Nth rows of the matrix store the coordinates of the start and end points, respectively, of the transmission line. The row indexes of this matrix can indicate the sequence of such points on the transmission line.

Then, we find the segment of the transmission line that is intercepted by the inner circle of the concentric ring. The point with the largest row index of the coordinate matrix on this intercepted segment can be identified. Note that this point is the one that is most close to the end point of the transmission line from the intercepted segment.

After that, we use this point as the center point and *r* as the radius to plot another circle. The intersection area of this new plotted circle and the intersection area I can be identified and defined as the candidate area where all the candidate nodes for the next location of receiver station deployment are located. Figure 3.6 shows such a candidate area.

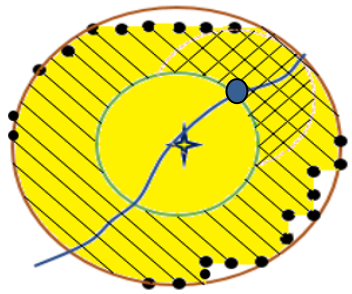

LEGEND
- Transmission line
- Receiver station
- *l* radius circle
- *u* radius circle
- Boundary
- Feasible region
- Intersection Area I
- Candidate nodes Area
- The point on the intercepted transmission line segment with the highest row index in the *N*x2 coordinate matrix

Figure 3.6. Candidate Area

When the candidate area is identified, all nodes in the candidate area can be identified as the candidate location for the next deployment of receiver station, *f* value will be calculated for each candidate node using (22).

$$f(n) = g(n) + h(n) + o(n) \tag{22}$$

In (2), $g(n)$ is the travel distance from the start point to candidate location n. $h(n)$ is the distance between the end point and candidate location n. $o(n)$ is the sum of the travel distance from candidate location n to all the obstacles in candidate area. The location for the next deployment will be identified by

$$n = \arg\min f(n) \tag{23}$$

$o(n)$ is used to model possible travel distance to deal with the obstacles. It is hoped that the location with the shortest travel distance when dealing with obstacles be selected to form the path. After using (2) and (3), the winner location for the next deployment of receiver station can be identified. On one hand, the winner may be the location of a certain obstacle. If this happens, the obstacle clearance and receiver station redeployment can be conducted simultaneously. On the other hand, the winner can also be the non-obstacle node. For those obstacles that are not selected as the new deployment location for the receiver station, the maintenance technician may need to take a round trip between the receiver station and the obstacle to implement a clearance. In Figure 3.7, the first and third obstacles illustrate such a possibility.

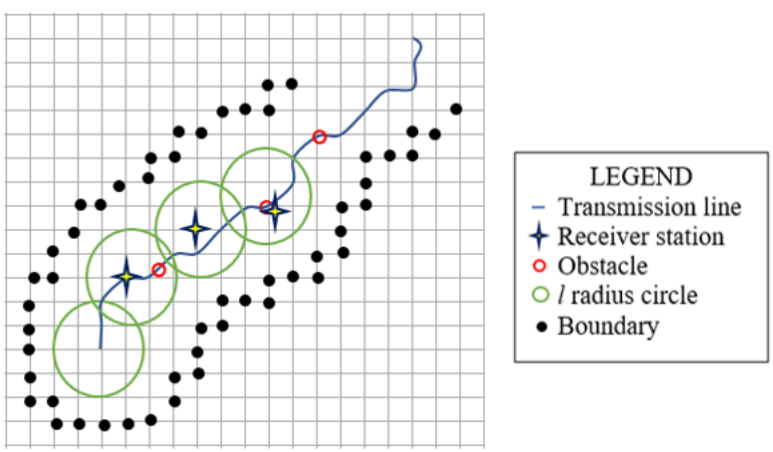

Figure 3.7. An Example to Illustrate the Obstacles and Next Location

The algorithm can be briefly described as follows.

0. Initialize the algorithm to obtain the required known conditions. Generate an $N\times2$ matrix to store the coordinates of the points on the transmission line according to a given resolution as well as the known obstacles.
1. Identify the feasible regions considering the constraint of data transmission range and the appropriateness for receiver station deployment.
2. The feasible region is then meshed into a set of grid nodes with a given resolution.
3. Find the candidate area where the candidate nodes can be located for the next deployment.
   - 3a. Plot two circles using the current location of receiver station as the center, r and $2r$ as radiuses, respectively so that a concentric ring with inside radius of r and outside radius of $2r$ can be formed.
   - 3b. Find the intersection area between the concentric ring plotted in step 3a and the feasible region defined in step 2. Call this intersection area as intersection area I.
   - 3c. Find the candidate area.
     - 3c-1. Find the segment of the transmission line that is intercepted by the inner circle of the concentric ring.
     - 3c-2. Choose the point from the segment obtained in step 3c-1 with a maximum row index in the coordinate matrix.
     - 3c-3. Use the point chosen in step 3c-2 as the center point and r as the radius to plot a circle. Find the intersection area between this circle and intersection area I and define this intersection area as candidate area.
   - 3d. Nodes obtained in step 2 as well as the obstacle nodes in the candidate area will be the candidate locations for the next deployment of successive receiver station.
4. Using equations (2) and (3) to determine the node for the next deployment location among all the candidate locations.
5. Set the winning node as the next location for receiver station deployment, repeat

steps 3 to 4 until any of the two terminating conditions described as follows is met.

Terminating condition 1: if the coordinate of the transmission line's end point becomes one of the candidate nodes, then it will be chosen as the last receiver station irrespective of the other nodes.

Terminating condition 2: if the coordinate of the transmission line's end point lies within the *r* radius circle of the current receiver station, then it will be chosen as the last receiver station.

By running the algorithm, all the deployment locations of the receiver stations can be identified to form the travel path of the ground team. The sum of the distance between each consecutive pairs of the deployment locations of receiver stations plus the distance between the first (last) receiver station and start (ending) point of the transmission line will be the total travel distance. Figure 3.8 shows the possible results. We can see that the center of each green circle forms the position for each receiver station deployment. Out of the four obstacles present, the 3rd obstacle is selected as the deployment location of the receiver station due to the lower *f* value compared to other candidate locations.

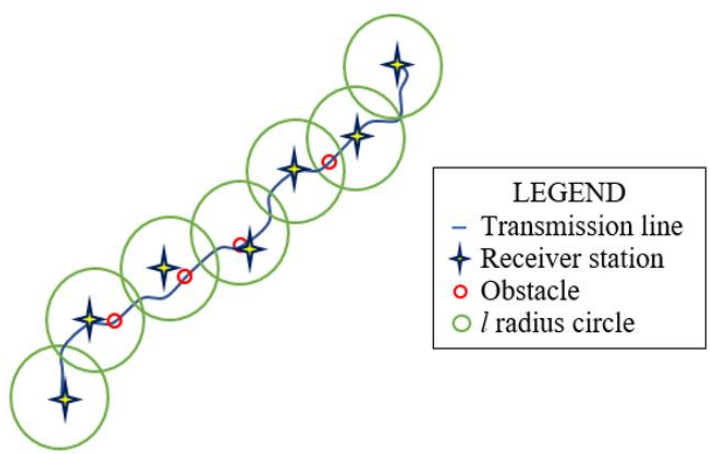

Figure 3.8. An Example of the Completion of the Algorithm to Cover the Entire Transmission Line

3.3. CASE STUDY

To illustrate the effectiveness of the proposed revised A-Star algorithm, a case study using a true segment of transmission line is conducted. The transmission line of 161 kV in Missouri (Ameren, 2017) as shown by an orange line in Figure 3.9 is used in the case study. The distance of this section of transmission line is 59 miles.

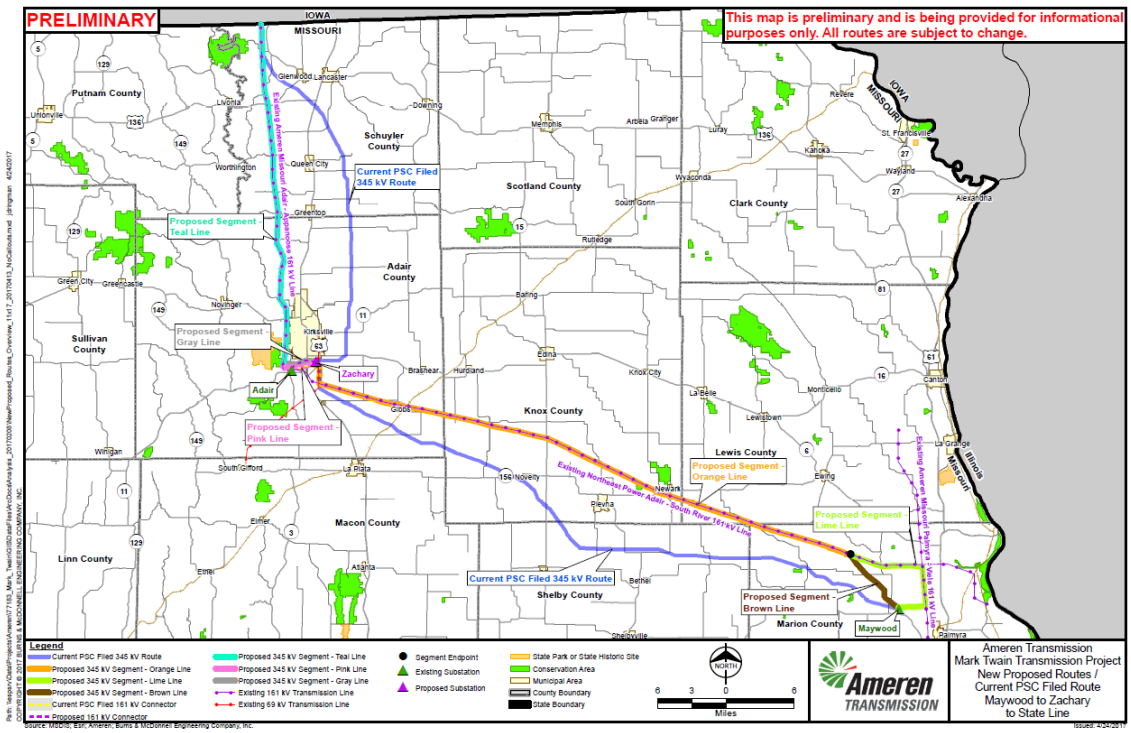

Figure 3.9. The Section of Transmission Line Used in Case Study

The GPS coordinate of this section of transmission line is obtained from the Figure 3.9. To make the obtained Coordinates more compatible with our proposed algorithm in Subsection 3.2, it is converted into Cartesian coordinate as shown in Figure 3.10.

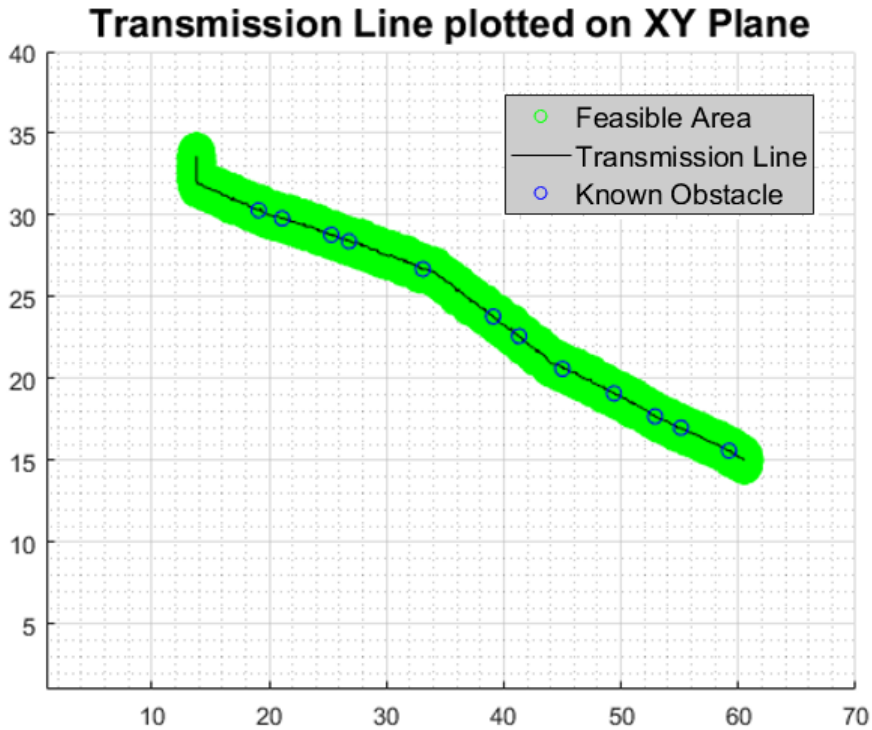

Figure 3.10. Transmission Line on a Cartesian Coordinate Plane

There are 12 obstacles, e.g., the structure lattice, large aerial marker, where human interference is needed to help robot for a clearance. The locations of these obstacles are shown in Table 3.1.

Table 3.1. Distance Between Obstacle and Start Point

Distance from starting Point (mile)	
Obstacle 1	1.81
Obstacle 2	6.68

Table 3.1. Distance Between Obstacle and Start Point (Cont.)

Obstacle 3	9.24
Obstacle 4	13.56
Obstacle 5	18.92
Obstacle 6	24.07
Obstacle 7	27.04
Obstacle 8	34.87
Obstacle 9	43.06
Obstacle 10	45.24
Obstacle 11	50.49
Obstacle 12	53.01

The robot battery change is hopefully to be conducted at the obstacle locations so that change of battery and obstacle clearance or receiver station redeployment can be conducted in the same time period to avoid additional travel. If the robot travel distance between two obstacles is beyond the battery capacity, a battery change between such pairs of obstacles is required. This battery change location is modeled as a “pseudo obstacle” in the algorithm. Table 3.2 shows the obstacles after considering battery change where obstacle 7’, obstacle 8’ and obstacle 12’ are three pseudo obstacles used for the battery change. The battery capacity is 1324 Wh (Montambault & Pouliot, 2012). The power for motion is 160 W (Montambault & Pouliot, 2012). The complete charge of the battery is not considered for calculating the location of the pseudo obstacles. Only 85% of the Battery charge is considered for a single charging/discharging cycle and rest 15% is stored for contingencies on the robot’s course of travel. The pseudo obstacles are considered when the robot reaches to a charge near to 0 Wh and there is no known obstacle nearby to consider for a change of battery.

Table 3.2. Obstacle Location for Battery Change

Distance from starting Point		Battery remaining capacity (Wh)	Battery Change?
Obstacle 1	1.81	835.8	No
Obstacle 2	6.68	56.6	Yes
Obstacle 3	9.24	715.8	No
Obstacle 4	13.56	24.6	Yes
Obstacle 5	18.92	267.8	Yes
Obstacle 6	24.07	301.4	Yes
Obstacle 7	27.04	650.2	No
Obstacle $7'$	31.10	0	Yes
Obstacle 8	34.87	522.9	No
Obstacle $8'$	38.13	1	Yes
Obstacle 9	43.06	336.6	Yes
Obstacle 10	45.24	776.6	Yes
Obstacle 11	50.49	285.4	Yes
Obstacle 12	53.01	722.2	No
Obstacle $12'$	57.52	0	Yes

The robot data transmission range is set to 1.3 miles. Using the proposed model introduced in Subsection 3.2, we find the travel route of the ground supporting team for relocating receiver stations as shown in Figure 3.11.

The known obstacles (aerial markers for example) and the pseudo obstacles are displayed in a distinct manner in Figure 3.11. In the later parts, results from the proposed methods mentioned in the current and previous sections are compared to check their effectiveness.

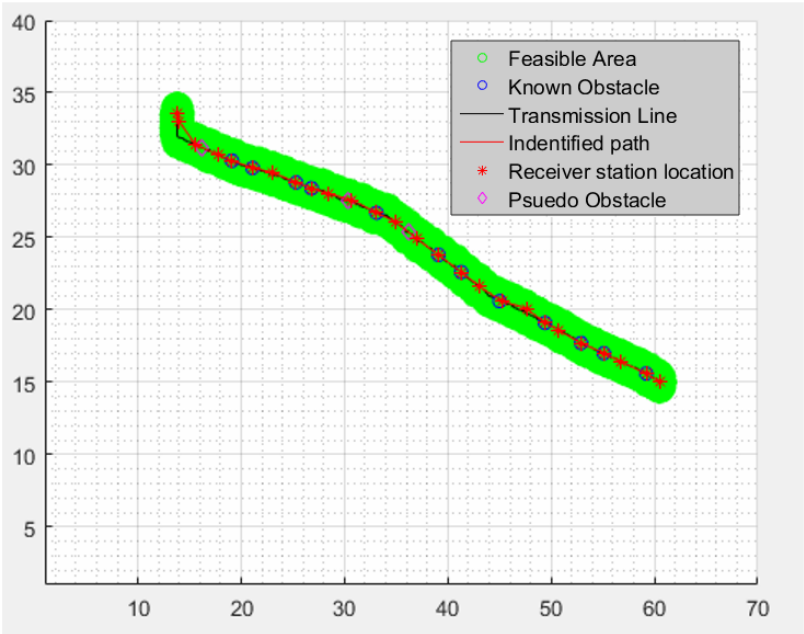

Figure 3.11. Deployment Location of Receiver Station

The comparison of the number of receiver station deployment between the proposed method and the method in Section 2 is summarized in Table 3.3. The number of receiver stations needs to be deployed is increased. This is mainly due to the fact that the method in Section 2 assumes there are no non-appropriate locations for deploying receiver stations and thus it can fully utilize the data transmission range of *r*.

Table 3.3. Comparison of Number of Receiver Stations

	Method in Section 2	Proposed Method	Reduction
Number of receiver stations	24	26	-8.33%

In addition, the time required for completing the inspection task is examined. First, we examine the time spent on the activities that can be controlled by the routing algorithm as shown in Table 3.4. Such activities include ground travel of the entire team for relocating receiver stations, ground travel of technician from receiver station to obstacle, obstacle clearance time, and setup time of receiver station due to multiple relocations of receiver station. We assume the speed of the truck carrying the entire team and receiver station is 20 miles per hour. The setup time of receiver station is assumed to be 24 minutes. The human interference time for clearing obstacle is set as 12 minutes per obstacle. In addition, we also assume that the robot is stopped during the periods when receiver station is relocated as well as the technician moves from receiver station to the obstacle location to help robot clear the obstacle. The comparison of the total time spent is illustrated in Table 3.5.

Table 3.4. Comparison of Controllable Time (h)

Activities	Method in Section 2	Proposed Method	Reduction
Travel time for relocating receiver station	3.03	2.55	15.9%
Receive station setup time	9.6	10.4	-8.33%
Obstacle clearance time	3	0.8	73.33%
Travel time from receiver station to real obstacle	0.21	0.1	52.33%
Travel time from receiver station to pseudo obstacle	0.13	0.08	40.71%
Total controllable time	15.97	13.93	12.80%

Table 3.5. Comparison of Total Time (h)

Activities	Method in Section 2	Proposed Method	Reduction
Travel time for relocating receiver station	3.03	2.55	15.9%
Initial Setup time	0.20	0.2	0%
Receiver station setup time	9.6	10.4	-8.33%
Obstacle clearance time	3	0.8	73.33%
Final closing time	3.00	3.00	0%
Travel time from receiver station to real obstacle	0.21	0.10	52.33%
Travel time from receiver station to pseudo obstacle	0.13	0.08	40.71%
Robot travel time	38.74	38.74	0%
Total time	57.91	55.86	3.53%

The travel time for relocating the receiver station can be significantly reduced. The obstacle clearance time and travel time from the receiver station to both real and pseudo obstacles are significantly reduced due to the fact that the obstacle clearance can be conducted during the same period for relocating receiver station. The time for receiver station set up for the redeployment is increased due to the increase in the number of receiver stations need to be deployed. The time that can be controlled by the routing algorithm is reduced by 12% although there exists an increase of receiver station set up time. The total time can be reduced by 3.5%.

Table 3.6. Cost Comparison ($)

Cost items	Method in Section 2	Proposed Method	Reduction
Battery depreciation	7.33	7.33	0%
Setup	275	88	68%
Robot depreciation	774.73	774.73	0%
Salary	5790.78	5586.30	3.53%
Data transmission system depreciation	13.58	12.87	5.22 %
Auxiliary equipment depreciation	38.03	36.05	5.22%
Ground travel	890.61	696.81	22.76%
Total Cost	7790.06	7202.09	7.55%

The cost comparison between the routing algorithm described Section 2 and the proposed method in this section is conducted. The cost model can be briefly described in Figure 2.5. The related parameters used in the comparison are provided in Tables 2.2, 2.4 and 2.5.

The total cost for such an inspection trip can be reduced by approximately 7% compared to the previous routing algorithm. This is mainly due to the reduction of the salary cost and ground travel cost, two largest contributors to the total cost. Ground travel cost is proportional to the ground travel distance, while salary cost is proportional to the time spent. Both can be effectively reduced by the proposed algorithm.

3.4. CONCLUSION

A considerable improvement by adopting the revised A-Star algorithm over the heuristic routing strategy described in Section 2 can be achieved. The travel costs of the ground team form a sizable portion of the total cost for the operation. The proposed A-Star

method primarily focuses on decreasing the travel distance of the ground team. The decrease in the total distance traveled results in the lesser time taken for the operation thereby, decreasing other costs such as the salary and other depreciation values. More considerations in the feasible area can be considered like forest area or a waterway using the proposed A-Star method thereby increasing the chances of getting a more realistic route.

4. CONCLUSION AND FUTURE WORK

In this thesis, we focus on the cost-effective analysis of using the suspended robot in transmission line inspection. A cost model is first established based on a simple heuristic routing algorithm to guide the motion of ground support team to ensure the robot is within the data transmission range and help robot clear the obstacles beyond the clearance capability. Then, a new routing algorithm is proposed based on a revised A-Star algorithm to further improve the cost-effectiveness when using the suspended robot in transmission line inspection through reducing the ground travel distance, travel time, and travel cost.

The thesis explores the economic feasibility of using the suspended robot in transmission line inspection. It offers a set of useful tools to guide the motion of ground supporting team when implementing the inspection. The research outcomes can provide initial insights in terms of utilizing the suspended robot in a transmission system routine inspection. It will help utility company better implement transmission system maintenance.

For future work, sensitivity analysis can be implemented to examine the influence of the variation of input parameters on the results to test the robustness of the proposed cost model. The real-time decision making for the situation that unexpected obstacles appear can be studied. The analytical model aiming at the optimal travel path with minimum travel time and/cost can be formulated and explored. In addition, the extension of the method for some other types of robot, e.g., aerial based robot, in transmission line inspection can be implemented. Also, another extension can be focused on the optimal decision making for deploying multiple teams with multiple robots for inspecting a certain network of a transmission line.

BIBLIOGRAPHY

Ameren (2017). Mark Twain Transmission Project. Retrieved from https://www.ameren.com/mark-twain/maps.

Beltran, H., Segundo, S., Fuster, V., Perez, L., & Mayorga, P. (2006). Automated Inspection of Electric Transmission Lines: The power supply system. *IECON 2006 - 32nd Annual Conference on IEEE Industrial Electronics.*

Boroujeni, Z., Goehring, D., Ulbrich, F., Neumann, D., & Rojas, R. (2017). Flexible Unit A-star Trajectory Planning for Autonomous Vehicle on Structured road maps. *Proceedings of the 2017 IEEE International Conference on Vehicular Electronics and Safety, June 27-28, 2017.*

Boyer, M. (1996). Systems integration in telerobotics: case study: maintenance of electric power lines. Proceedings of IEEE International Conference on Robotics and Automation.

Campos, M., Pereira, G., Vale, S., Bracarense, A., Pinheiro, G., & Oliveira, M. (2002). A mobile manipulator for installation and removal of aircraft warning spheres on aerial power transmission lines. Proceedings 2002 IEEE International Conference on Robotics and Automation (Cat. No.02CH37292).

Conradie, P., Dimitrov, D., & Oosthuizen, G. (2016). A cost modelling approach for milling titanium alloys. *Procedia cirp*, *46*, 412-415.

Dave, B. (n.d.). *Resource Adequacy and Transmission Security of the Bulk Power System - Utility Products Magazine*. Retrieved from http://www.utilityproducts.com/articles/print/volume-16/issue-10/product-focus/transmission-distribution/resource-adequacy-and-transmission-security.html.

Debenest, P., Guarnieri, M., Takita, K., Fukushima, F., Hirose, S., Tamura, K., Kimura, A., Kubokawa, H., Iwama, N., & Shiga, F. (2008). Expliner – Robot for inspection of transmission lines. *Proceedings of 2008 IEEE International Conference on Robotics and Automation Pasadena, CA, USA, May 19-23, 2008.*

Debenest, P., & Guarnieri, M. (2010). Expliner — From prototype towards a practical robot for inspection of high-voltage lines. *Proceedings of 2010 1st International Conference on Applied Robotics for the Power Industry*.

DOE (U.S. Department of Energy), 2005, Tucson Electric Power Company Sahuarita-Nogales Transmission Line Final Environmental Impact Statement, DOE/EIS-0336, Office of Fossil Energy, U.S. Department of Energy, January.

Edkins, K. (2008). *Cable spacer-damper on power lines*. Retrieved from http://www.geograph.org.uk/photo/970517.

Elizondo, D., Gentile, T., Candia, H., & Bell, G. (2010). Overview of Robotic Applications for Energized Transmission Line Work –Technologies, Field Projects and Future Developments. *Proceedings of 2010 1st International Conference on Applied Robotics for the Power Industry Delta Centre-Ville Montréal, Canada, October 5-7, 2010.*

Faucher, D., Lessard, J., Rondot, P., Cote, J., & McGee, J. (1996). Ground operated teleoperation system for live power line maintenance. 1996 IEEE International Conference on Systems, Man and Cybernetics.

Goldberg, A. (2007). Point-to-point shortest path algorithms with preprocessing. *Sofsem*,9-12.

Groover, M. P. (2008). *Automation, production systems, and computer-integrated manufacturing*. Upper Saddle River: Prentice Hall.

How Electricity Is Delivered To Consumers - Energy Explained, Your Guide To Understanding Energy - Energy Information Administration. (n.d.). Retrieved from https://www.eia.gov/energyexplained/index.cfm?page=electricity_delivery

Hydro-Québec and National Grid Sign a Licensing Agreement for the LineScout Technology. (2014, September 14). Retrieved from http://www.tdworld.com/projects-progress/hydro-qu-bec-and-national-grid-sign-licensing-agreement-linescout-technology.

Jiang, L., Walczyk, D., McIntyre, G., & Chan, W. K. (2016). Cost modeling and optimization of a manufacturing system for mycelium-based biocomposite parts. *Journal of Manufacturing Systems, 41*, 8-20.

Koike, M., Kurabe, K., Yamashita, K., Kato, Y., Jinno, K., & Tatsuno, K. (2016). An approach to object recognition for a power distribution line maintenance robot. The case of identifying a mechanical bolt to be tightened with a nut. 2016 International Symposium on Micro-NanoMechatronics and Human Science (MHS).

Liu, S., Cruzat, C., & Kopsidas, K. (2017). Impact of transmission line overloads on network reliability and conductor ageing. 2017 IEEE Manchester PowerTech.

Liu, T., & Zhang, Q. (2017). Grid-connected/island optimal operation of PV-diesel-battery microgrid with plug-in electric vehicles. *Proceedings of 32nd Youth Academic Annual Conference of Chinese Association of Automation*.

Molburg, J. C., Kavicky, J. A., & Picel, K. C. (2008). The design, construction, and operation of long-distance high-voltage electricity transmission technologies.

Montambault, S., & Pouliot, N. (2003). The HQ LineROVer: contributing to innovation in transmission line maintenance. *2003 IEEE 10th International Conference on Transmission and Distribution Construction, Operation and Live-Line Maintenance, 2003. 2003 IEEE ESMO.*

Montambault, S., Paouliot, N., Toth, J., & Spalteholz, B. (2010). Reporting on a Large Ocean Inlet Crossing Live Transmission Line Inspection Performed by LineScout Technology. *Proceedings of the 2010 IEEE International Conference on Robotics and Automation Anchorage Convention District May 3-8, 2010, Anchorage, Alaska, USA.*

Montambault, S., & Pouliot, N. (2010). Field experience with LineScout Technology for live-line robotic inspection and maintenance of overhead transmission networks. 2010 1st International Conference on Applied Robotics for the Power Industry (CARPI 2010).

Montambault, S., & Pouliot, N. (2012). Field-oriented developments for LineScout technology and its deployment on large water crossing transmission lines. *Journal of Field Robotics, 29*(1), 25-46.

Montambault, S., Pouliot, N., & Lepage, M. (2012). On the latest field deployments of LineScout Technology on live transmission networks. 2012 2nd International Conference on Applied Robotics for the Power Industry (CARPI).

Muratori, M., Ledna, C., McJeon, H., Kyle, P., Patel, P., Kim, S. H., et al. (2017). Cost of power or power of cost: A U.S. modeling perspective. *Renewable and Sustainable Energy Reviews, 77*, 861-874.

Nagarajan, B., Qin, R., Sun, Z., & Islam, M. (2017). Cost analysis for high voltage transmission line inspection using robot. *Proceedings of the American Society for Engineering Management 2017 International Annual conference 18-21 Oct. 2017.* Copyright © 2017. Reprinted with permission of the American Society for Engineering Management. International Annual Conference. All rights reserved.

Ortega-Vazquez, M.A. (2013). Optimal scheduling of electric vehicle charging and vehicle-to-grid services at household level including battery degradation and price uncertainty. Published in IET Generation, Transmission & Distribution.

Overhead Distribution Manual. (n.d). *Preformed* [Online]. Available: http://www.preformed.com/images/pdfs/Energy/Transmission/Motion_Control/Detuning_Pendulum/EN-TM-1002-4_DistRepairwBleed.pdf.

Overhead Line Splices Automatic Copper. (n.d.). Retrieved from http://www.hubbellpowersystems.com/catalogs/connectors/DB.pdf.

Peterson, S.B., Apt, J., & Whitacre, J.F. (2010). Lithium-ion battery cell degradation resulting from realistic vehicle and vehicle-to-grid utilization. *Journal of Power Sources, 195*(8), 2385–2392.

Peungsungwal, S., Pungsiri, B., Chamnongthai, K., & Okuda, M. (2001). Autonomous robot for a power transmission line inspection. ISCAS 2001. The 2001 IEEE International Symposium on Circuits and Systems (Cat. No.01CH37196).

Phillips, A., Engdahl, E., McGuire D., Major M., & Bartlett G. (2012). Autonomous overhead transmission line inspection robot (TI) development and demonstration. Proceedings of 2012 2nd International Conference on Applied Robotics for the Power Industry (CARPI).

Pouliot, N., Richard, P., & Montambault, S. (2006). LineScout Technology: Development of an inspection robot capable of clearing obstacles while operating on a live line. *Proceedings of ESMO 2006 - 2006 IEEE 11th International Conference on Transmission & Distribution Construction, Operation and Live-Line Maintenance 15-19 Oct. 2006.*

Pouliot, N., & Montambault, S. (2008). Geometric design of the LineScout, a teleoperated robot for power line inspection and maintenance. 2008 IEEE International Conference on Robotics and Automation.

Pouliot, N., Latulippe, P., & Montambault, S. (2009). Reliable and intuitive teleoperation of LineScout: a mobile robot for live transmission line maintenance. 2009 IEEE/RSJ International Conference on Intelligent Robots and Systems.

Pouliot, N., & Montambault, S. (2009). LineScout Technology: From inspection to robotic maintenance on live transmission power lines. 2009 IEEE International Conference on Robotics and Automation.

Pouliot, N., Mussard, D., & Montambault, S. (2012). Localization and archiving of inspection data collected on power lines using LineScout Technology. 2012 2nd International Conference on Applied Robotics for the Power Industry (CARPI).

Pouliot, N., Richard, P., & Montambault, S. (2015). LineScout technology opens the way to robotic inspection and maintenance of high-voltage power lines. *IEEE Power and Energy Technology Systems Journal, 2*(1), 1-11.

Rego, C., Santos, C., & Conceicao, E. N. (2014). Application of high voltage (HV) live-line working techniques - Hot stick in HV/MV substation maintenance -A case study. *2014 11th International Conference on Live Maintenance (ICOLIM).*

Richard, P., Pouliot, N., & Montambault, S. (2014). Introduction of a LIDAR-based obstacle detection system on the LineScout power line robot. 2014 IEEE/ASME International Conference on Advanced Intelligent Mechatronics.

Roncolatto, R. A., Romanelli, N.W., CPFL-Paulista, Hirakawa, A., Horikawa, O., Vieira, D.M., Yamamoto, R., Finotto, V.C., Sverzuti, V., & Lopes. I.P. (2010). Robotics applied to work conditions improvement in power distribution lines maintenance. *Applied Robotics for the Power Industry (CARPI), Proceedings of 2010 1st International Conference on Applied Robotics for the Power Industry.*

Sawada, J., Kusumoto, K., Maikawa, Y., Munakata, T., & Ishikawa, Y. (1991). A mobile robot for inspection of power transmission lines. *IEEE Transactions on Power Delivery*, *6*(1), 309-315.

Song, Y., Wang, H., Jiang, Y., & Ling, L. (2012). AApe-D: A novel power transmission line maintenance robot for broken strand repair. *2012 2nd International Conference on Applied Robotics for the Power Industry (CARPI).*

The parts of a power line. (n.d.). Retrieved from http://www.emfs.info/sources/overhead/parts/.

Thrash, F.R., 2003, "Transmission Conductors — A Review of the Design and Selection Criteria." Available at http://www.southwire.com. Accessed September 12, 2006.

Toth, J., Pouliot, N., & Montambault, S. (2010). Field experiences using LineScout Technology on large BC transmission crossings. 2010 1st International Conference on Applied Robotics for the Power Industry (CARPI 2010).

Vetter, J., Novak, P., Wagner, M.R., Veit, C., Moller, K.C., Besenhard, J.O., Winter, M., Wohlfahrt-Mehrens, M., Vogler, C., & Hammouche, A. (2005). Ageing mechanisms in lithium-ion batteries. *Journal of Power Sources, 147*(1-2), 269–281.

Vibration Damper for Transmission Lines. (n.d.). Retrieved from http://www.hubbellpowersystems.com/literature/connectors/TB-203.pdf.

Wu, G., Zheng, T., Xiao, H., & Li, C. (2009). Navigation, location and non-collision obstacles overcoming for high-voltage power transmission-line inspection robot. 2009 International Conference on Mechatronics and Automation.

Zhang, Z., Wang, J., & Cao, X. (2014). Economic dispatch of microgrid considering optimal management of lithium batteries. *Proceedings of 2014 International Conference on Power System Technology*.

Zhang, Z., Wang, J., & Wang, X. (2015). An improved charging/discharging strategy of lithium batteries considering depreciation cost in day-ahead microgrid scheduling. *Energy Conversion and Management, 105*, 675-684.

VITA

Balaji Rathinam Nagarajan was born in Theni, Tamil Nadu, India. Nagarajan received his Bachelor degree in Mechanical Engineering from one of India's leading private university, Shiv Nadar University, Noida, India, in May 2015. He came to Missouri University of Science and Technology in January 2016 to pursue his Master degree in Engineering Management. He joined the research team as a Graduate Research Assistant under the supervision of Dr. Zeyi Sun in September 2016. In the later semesters, he co-authored in two papers based on the project titled "A Survey of Robotics Technology Used by Utility Companies for Costs Reduction" funded by Ameren. The first one titled "Cost Analysis for High Voltage Transmission Line Inspection Using Robot" is published in the proceedings of ASEM annual conference of 2017. The second one titled "A Revised A-Star Algorithm to Identify the Travel Path and Receiver Station Deployment Location for Transmission Line Inspection Using Robot" has been submitted to Engineering Management Journal. He received his Master of Science degree in Engineering Management from Missouri University of Science and Technology in May 2018.